Published OnlineFirst January 21, 2014; DOI: 10.1158/1535-7163.MCT-13-0199

Molecular Cancer Therapeutics

Rationale and Preclinical Efficacy of a Novel Anti-EMP2 Antibody for the Treatment of Invasive Breast Cancer

Maoyong Fu, Erin L. Maresh, Gustavo F. Helguera, et al.

Mol Cancer Ther 2014;13:902-915. Published OnlineFirst January 21, 2014.

Published OnlineFirst January 21, 2014; DOI: 10.1158/1535-7163.MCT-13-0199

Molecular Cancer Therapeutics

Rationale and Preclinical Efficacy of a Novel Anti-EMP2 Antibody for the Treatment of Invasive Breast Cancer

Maoyong Fu[1], Erin L. Maresh[1], Gustavo F. Helguera[2,9], Meagan Kiyohara[1], Yu Qin[3], Negin Ashki[3], Tracy R. Daniels-Wells[2], Najib Aziz[1], Lynn K. Gordon[3,6], Jonathan Braun[1,5], Yahya Elshimali[7], Robert A. Soslow[8], Manuel L. Penichet[2,4,5], Lee Goodglick[1,5], and Madhuri Wadehra[1,5]

Abstract

Despite significant advances in biology and medicine, the incidence and mortality due to breast cancer worldwide is still unacceptably high. Thus, there is an urgent need to discover new molecular targets. In this article, we show evidence for a novel target in human breast cancer, the tetraspan protein epithelial membrane protein-2 (EMP2). Using tissue tumor arrays, protein expression of EMP2 was measured and found to be minimal in normal mammary tissue, but it was upregulated in 63% of invasive breast cancer tumors and in 73% of triple-negative tumors tested. To test the hypothesis that EMP2 may be a suitable target for therapy, we constructed a fully human immunoglobulin G1 (IgG1) antibody specific for a conserved domain of human and murine EMP2. Treatment of breast cancer cells with the anti-EMP2 IgG1 significantly inhibited EMP2-mediated signaling, blocked FAK/Src signaling, inhibited invasion, and promoted apoptosis *in vitro*. In both human xenograft and syngeneic metastatic tumor monotherapy models, anti-EMP2 IgG1 retarded tumor growth without detectable systemic toxicity. This antitumor effect was, in part, attributable to a potent antibody-dependent cell-mediated cytotoxicity response as well as direct cytotoxicity induced by the monoclonal antibody. Together, these results identify EMP2 as a novel therapeutic target for invasive breast cancer. *Mol Cancer Ther; 13(4); 902–15. ©2014 AACR.*

Introduction

Over the last decade, several advances have been made in the diagnosis and treatment of breast cancer, centered on the expression of specific molecular markers. Breast cancer is now divided into three major subtypes: tumors expressing estrogen receptors (ER) and/or progesterone receptors [PR; commonly referred to as hormone receptor–positive (HR-positive)], *ERBB2* [also known as human epidermal receptor 2 (*HER2/neu*)] amplified, and tumors lacking the expression of ERs and PRs and normal or negative HER2/neu expression termed triple-negative breast cancer (TNBC; refs. 1–4). Although this grouping has led to targeted therapies for some subtypes, in particular HR-positive and HER2-positive tumors, breast cancer still remains the most common malignancy and second deadliest among women worldwide (5). It is currently estimated that up to 30% of women with invasive breast cancer will eventually die from it, necessitating the need to identify new markers for therapy (6).

Recently, epithelial membrane protein-2 (EMP2) was identified as a novel prognostic indicator in a number of gynecologic cancers (7–9). Belonging to the growth arrest specific-3 (GAS3) family of tetraspan proteins, elevated EMP2 levels have been observed in advanced ovarian and endometrial tumors (7, 8), and its expression inversely correlated with endometrial cancer patient survival (9). This effect could be recapitulated through xenograft modeling as endometrial tumors where EMP2 expression was increased showed enhanced tumor growth (10). Furthermore, these tumors showed an addiction to EMP2 expression as they failed to efficiently form when EMP2 levels were suppressed (10, 11). Although limited information is known about its direct cellular function, previous studies have implicated EMP2 in the activation of focal adhesion kinase (FAK) and Src kinase in a number of cell types (12–15). Consistent with this putative mechanism, increased EMP2 levels correlated with an increase in cellular migration as well as neoangiogenesis in a FAK- and Src-dependent manner (10, 11).

Authors' Affiliations: Departments of [1]Pathology and Laboratory Medicine, [2]Surgery, Division of Surgical Oncology, [3]Ophthalmology, and [4]Microbiology, Immunology, and Molecular Genetics, and [5]Jonsson Comprehensive Cancer Center, David Geffen School of Medicine at UCLA; [6]Department of Surgery, Greater Los Angeles Veterans Affairs Healthcare System; [7]Department of Pathology, Charles Drew University, Los Angeles, California; [8]Department of Pathology, Memorial Sloan-Kettering Cancer Center, New York, New York; and [9]Institute of Experimental Biology and Medicine, University of Buenos Aires, Buenos Aires, Argentina

Note: Supplementary data for this article are available at Molecular Cancer Therapeutics Online (http://mct.aacrjournals.org/).

Corresponding Authors: Madhuri Wadehra, Department of Pathology and Laboratory Medicine, Box 951732, David Geffen School of Medicine at UCLA. Phone: 310-825-1590; Fax: 310-825-5674; E-mail: mwadehra@mednet.ucla.edu; and Lee Goodglick, Department of Pathology and Laboratory Medicine, Box 951732, David Geffen School of Medicine at UCLA. Phone: 310-825-825-9134; E-mail: lgoodglick@mednet.ucla.edu.

doi: 10.1158/1535-7163.MCT-13-0199

Published OnlineFirst January 21, 2014; DOI: 10.1158/1535-7163.MCT-13-0199

Recent studies examining global gene signatures identified upregulation of EMP2 mRNA in breast cancers, providing the first hint of dysregulated EMP2 expression in this malignancy (16–18). These studies suggested that EMP2 message positively correlated with advanced disease as well as identified circulating breast tumor cells (17, 19). In the present study, we examined the protein expression and frequency of EMP2 in human invasive breast cancers with an emphasis on triple-negative disease. Given its high membrane expression, we hypothesized that EMP2 may serve as novel target for therapy, and consistent with this idea, anti-EMP2 antibody fragments (diabodies) resulted in reduced tumor growth in both endometrial and ovarian cancer models (7, 20). To further the use of anti-EMP2 therapy, we created a novel fully human anti-EMP2 immunoglobulin G1 (IgG1) antibody and characterized its therapeutic potential. Collectively, our data suggest that anti-EMP2 therapy may be a first-in-class antibody to potentially treat aggressive breast cancers.

Materials and Methods

Tissue microarray

Tumor samples were collected as approved and monitored by the UCLA Institutional Review Board, and appropriate permission has been granted for use of the deidentified clinical data. A breast cancer tissue array (TMA) was constructed using archival breast tissue samples from 212 patients who had breast surgery at the UCLA Medical Center between 1995 and 2000 as previously described (21, 22). The samples examined were histopathologies from women who underwent surgery for breast cancer. In this study, 74 cases were examined (Supplementary Table S1) of which on average, each histopathology was represented by at least three cores. Some cases contained multiple histopathologies. For this study, we focused on the categories of normal glandular/ductal epithelium ($n = 139$ spots), ductal hyperplasia ($n = 35$ spots), ductal carcinoma *in situ* (DCIS; $n = 142$ spots), invasive ductal carcinoma ($n = 236$ spots), and lymph node metastatic lesions ($n = 69$ spots). The TMA was evaluated for EMP2 expression as described below. A blinded semiquantitative integrated scoring of the intensity and frequency of EMP2 staining was performed by two independent pathologists (R.A. Soslow and Y. Elshimali) as described previously (21, 22). The following formula (H score) was used to derive the integrated value: $[3(\%a) + 2(\%b) + 1(\%c]/100$, where a, b, and c are the percentages of cells staining at intensities 3, 2, and 1, respectively. Statistical analyses have been described previously and are presented below (21, 22).

Additional TNBC cases

Twenty-three TNBC tumors from an additional 23 individuals were stained for EMP2 as detailed below. Tumors were characterized as (i) no expression/below the level of detection (H score $= 0$); (ii) weak expression ($1 \leq H$ score > 0); and (iii) strong expression (H score ≥ 2).

Construction and expression of anti-EMP2 IgG1

We have previously described the construction of anti-EMP2 diabodies KS83 and KS49. For studies described here, we constructed a fully human anti-EMP2 IgG1 antibody. To do this, the diabody variable (V) region sequences of KS49 were obtained by PCR (20) and then cloned into the pCR-II-TOPO vector (Life Technologies). The cloning was confirmed by sequencing.

Variable heavy sequence

ATGGCCCAGGTGCAGCTGGTGGAGTCTGGGGG-AGGCTTGGTCCAGCCTGGGGGGTCCCTGAGACTC-TCCTGTGCAGCCTCTGGATTCACCTTCAGTAGCTA-TGCTATGCACTGGGTCCGCCAGGCTCCAGGCAAG-GGGCTGGAGTGGGTGGCAGTTATATCATATGATG-GAAGCAATAAATACTACGCAGACTCCGTGAAGG-GCCGATTCACCATCTCCAGAGACAATTCCAAGAA-CACGCTGTATCTGCAAATGAACAGCCTGAGAGCT-GAGGACACGGCTGTGTATTACTGTGCCCGAACAG-TGGGAGCTACTGGAGCTTTTGATATCTGGGGCCA-AGGGACAATGGTCACCGTCTCG.

Variable light sequence

GACATCGTGATGACCCAGTCTCCTTCCACCGTG-TCTGCTTCTGTAGGAGACAGAGTCATCATCCCTTG-CCGGGCCAGTCAGAGTATTGGTAAGTGGTTGGCC-TGGTATCAGCAGAAACCAGGGAAAGCCCCAAAA-CTCCTGATCTATAAGGCGTCTAGTTTAGAAGGTTG-GGTTCCATCAAGGTTCAGCGGCAGTGGGTCTGGG-ACAGAATTCTCTCTCACCATCAGTAGCCTGCAGCC-TGACGATTCTGCAACTTATGTCTGTCAACAGTCTC-ACAATTTCCCTCCCACTTTCGGCGGAGGGACCAA-GCTGGAGATCAAACGTGCGGCCGCAGAACAAAA-ACTCATCTCAGAAGAGGATCTGAATGGGGCCGC-A.

The sequence contains a functional signal peptide for proper secretion, and they were inserted into the κ light chain and γ1 heavy chain IgG1 expression vector using *Eco*RV and *Sal*I or *Eco*RV and *Nhe*I sites, respectively. These vectors contain the cytomegalovirus promoter (CMV) and have been shown to secrete functional recombinant antibodies in murine myeloma cells (23). Both expression vectors were provided by Dr. Sheri Morrison (University of California, Los Angeles). The heavy and light chain expression vectors were transfected into CHO-K1 cells as described previously (24). Cells were then screened by ELISA (described below) using goat anti-human IgG (Life Technologies) and goat anti-human κ chain (Sigma-Aldrich). The five highest producing subclones were isolated to use for S-35 biosynthetic antibody labeling and immunoprecipitation with hyperimmune rabbit antihuman IgG (Sigma-Aldrich) and Staph A (IgGSorb; The Enzyme Center), to validate and select the optimal clone. The best producer was expanded into roller bottles to maximize the secretion of antibodies (25). After 2 to 3 weeks, supernatants were collected and filtered for purification as below.

Supernatants were passed over a 1.5 mL volume FlexColumn (Thermo Fisher Scientific) with 1 mL of

Published OnlineFirst January 21, 2014; DOI: 10.1158/1535-7163.MCT-13-0199

protein A-Sepharose (Sigma-Aldrich), and bound proteins were eluted with 2 column volumes of 0.2 mol/L citrate buffer (pH 4.5), 3 column volumes of 0.1 mol/L glycine-HCl (pH 2.5) and 2 column volumes of 0.1 mol/L glycine-HCl (pH 2.0), sequentially. The eluted fractions containing the desired antibodies were dialyzed against PBS with Slide-A-Lyzer Dialysis Cassettes (Thermo Fisher Scientific). The final concentration of purified antibodies was measured with NanoDrop 2000 (Thermo Scientific).

ELISA

Biotinylated 24-amino acid peptides corresponding to the extracellular loop of human EMP2 (20) were coated onto streptavidin-coated 96-well plates (Roche Applied Science). ELISA was performed as described previously (20). Specifically, bound antibodies were detected with horseradish peroxidase (HRP)–conjugated goat anti-human IgG (Jackson ImmunoResearch) and TMB solution (eBioscience). Absorbance at 450 nm was determined using a microplate reader Model 550 (Bio-Rad).

Flow cytometry

EMP2-positive cells (HEC1a/EMP2, HEC1a, (15) or 4T1 cells) or EMP2-negative cells (EL4 or Ramos) were resuspended at a concentration of 10^6 cells in 1 mL of cold PBS + 0.2% BSA buffer (flow buffer). The cell suspension was centrifuged for 5 minutes at 500 $\times g$, at 4°C. Cells were then incubated with 1 μg of recombinant anti-EMP2 IgG1 for 2 hours at 4°C. An IgG specific for the hapten dansyl, 5-dimethylamino naphthalene-1-sulfonyl chloride (DNS) was used as a nontargeted antibody negative control (26). Cells were washed three times and then incubated for 30 minutes at 4°C with phycoerythrin (PE)-conjugated goat anti-human IgG (Jackson Immunoresearch). Cells were washed and resuspended in flow buffer. Flow cytometry was immediately performed with a Becton Dickinson FACScan analytic flow cytometer (Becton Dickinson) in the UCLA Jonsson Comprehensive Cancer Center and Center for AIDS Research Flow Cytometry core facility.

Immunohistochemistry

Immunohistochemistry (IHC) for human EMP2 expression has been described previously (9). Briefly, following antigen retrieval, slides were incubated with rabbit anti-human EMP2 antisera (1:400) for 1 hour. In some experiments, the anti-EMP2 IgG1 was used to detect EMP2 in normal and tumor tissue (Supplementary Figure 1); a detailed protocol is provided in the Supplementary Material. Samples were then incubated with biotinylated goat anti-rabbit secondary antibody and then streptavidin HRP from the VECTASTAIN Elite ABC Kit (Vector Labs). The antibody was detected using the Vector Labs DAB Substrate Kit (Vector Labs) following the manufacturer's protocol. Negative controls included preimmune serum incubation.

Cell lines and cell culture

Human breast cancer cell lines HS578t, BT-474, SK-BR-3, MCF7, UACC812, BT-20, MDA-MB-231, ZR-75-1, and MDA-MB-468 (American Type Culture Collection, ATCC) were cultivated in Dulbecco's Modified Eagle Medium (DMEM; Mediatech) supplemented with 10% fetal calf serum (FCS; Hyclone Laboratories), 2 mmol/L L-glutamine, 1 mmol/L sodium pyruvate, 100 U/mL penicillin, and 100 U/mL streptomycin (all from Life Technologies). All cell lines were used within 6 months of resuscitation and were characterized by the cell bank. Cells were cultured at 37°C in a humidified 5% CO_2. 4T1 cells, a spontaneous mammary tumor syngeneic in BALB/c mice, were obtained from ATCC. 4T1 cells were maintained in RPMI medium supplemented as above, and the cells were infected with firefly luciferase (FLUC) by the Jonsson Comprehensive Cancer Center (JCCC) Viral Vector Core Laboratory. In addition, HS578t, MDA-MB-231, MDA-MB-468, and SK-BR-3 sublines were prepared that overexpress EMP2 as previously described (15). Cell lines bearing an empty expression vector were also produced as described (15). Cell lines were also prepared with reduced EMP2 expression through stable infection using an EMP2-specific short hairpin RNA (shRNA; TRCN0000322911) in pLKO.1-puro (Sigma-Aldrich). Stably infected breast cancer cells containing a nontargeting shRNA control were also created. Cell lines were used within 6 months after selection. Western blot analysis was used to confirm the EMP2 expression levels in each cell line (see below). Cell lines were passaged in our laboratory for less than 6 months.

Western blot analysis

Preparation of breast cancer cell lines or tissue lysates for Western blotting has been described previously (8). Cells were lysed in Laemmli buffer and, for EMP2 detection, were treated with N-glycosidase F (New England Biolabs) to remove N-link glycosylation (15). Proteins were separated using SDS-PAGE, transferred onto nitrocellulose membrane and blocked in 10% nonfat dry milk in TBS-Tween-20 buffer. Blots were probed using rabbit anti-human EMP2 antisera (1:2,000; ref. 27). Proteins were then detected by using a HRP-conjugated goat anti-rabbit antibody. As a loading control, β-actin expression was detected using primary monoclonal anti-β actin (Sigma) and secondary HRP-conjugated goat anti-mouse IgG (Amersham). Bands were visualized using ECL detection reagents (Amersham).

In some experiments, MDA-MB-468 cells were treated for 2 hours with 100 μg/mL of anti-EMP2 IgG1 or control IgG. Cells were then plated to activate FAK and Src and then lysed after 12 hours (28, 29). Separated proteins were probed using anti- 576/577p-FAK (Santa Cruz Biotechnology), anti- total FAK (BD Biosciences), anti-416 p-Src (Cell Signaling Technology), anti-total Src (Cell Signaling Technology) or β-actin (Sigma-Aldrich).

Published OnlineFirst January 21, 2014; DOI: 10.1158/1535-7163.MCT-13-0199

Invasion assays

Of note, 24-well plates with Transwell inserts were used to perform the *in vitro* cell invasion assays. Equivalent numbers (5×10^3 cells) of MDA-MB-231 breast cancer cells with modified EMP2 levels were added to the top chamber of the Transwell, and complete DMEM was added to the bottom of the well. Cells were allowed to invade for 6 hours at 37°C. The filters were then fixed and stained with 0.1% crystal violet. The invasive cells were visualized using bright-field microscopy. Cells were enumerated by counting four random fields per Transwell. The experiment was repeated three times, with the data averaged. In some experiments, cells were pretreated with anti-EMP2 IgG1 or control antibodies for 2 hours at 4°C.

ADCC assays

Peripheral blood mononuclear cells (PBMC) were isolated from blood using Ficoll-Paque PLUS (GE Healthcare) from 3 volunteers. Blood donors had given informed consent before for obtaining a peripheral venous blood sample for PBMC assays. These experiments were done according to the rules of the Ethical Committee of University of California, Los Angeles. PBMCs were resuspended in DMEM with 10% FCS. SK-BR-3 cells were initially labeled using PKH67 fluorescent dye (Sigma-Aldrich) and then plated in 6-well plates. Cells were preincubated with anti-EMP2 IgG1 or trastuzumab (anti-HER2/*neu*; Genentech) as a positive control overnight and then incubated with different ratios of PBMCs for 4 to 8 hours at 37°C. The percentage of cell death was quantitated by propidium iodide staining using a Becton Dickinson FACScan analytic flow cytometer (Becton Dickinson) at the UCLA JCCC and Center for AIDS Research Flow Cytometry core facility. Experiments were performed in duplicates, normalized to an untreated negative control, and then averaged.

Viability assays

Cells (5×10^4) were placed in triplicate in a 6-well plate (Becton Dickinson) and incubated with anti-EMP2 diabody KS83 (15, 20), control diabody A10 (20), anti-EMP2 IgG1, control IgG (Sigma-Aldrich), or a saline control as indicated in the figure legends for 24 to 96 hours. Cells were then harvested, and the number of viable cells relative to the initial plating (% growth) was determined using a trypan blue exclusion assay. To assess whether resultant cell death was due to apoptosis, cells were harvested and stained with an Annexin V-FITC Detection Kit according to manufacturer's instructions (BD Biosciences). Flow cytometry was performed as above.

To confirm cell viability on a larger panel of cells, the CellTiter-Glo Luminescent Cell Viability Assay (Promega) was performed according to manufacturer instructions. Cells (5×10^3) were seeded in 96-well plates and then treated with 0 to 250 μg/mL anti-EMP2 IgG1 or control antibodies for 3 to 5 days. The luminescence was quantitated on a microplate reader (FLUOstar OPTIMA).

Pharmacokinetic analysis

To determine the half-life of the anti-EMP2 IgG1 in mice, pharmacokinetic studies were performed. A detailed protocol is described in the Supplementary Methods.

In vivo toxicity

All mouse experiments were performed under protocols approved by the Chancellor's Animal Research Committee at UCLA, and animals were maintained in accordance with the National Academy of Science Guide for the Care and Use of Laboratory Animals in the Vivarium of UCLA. We tested for potential systemic toxicity by recombinant anti-EMP2 IgG1 in 7-week-old female wild-type (C57BL/6) mice obtained from The Jackson Laboratory. At least three animals per group were injected intraperitoneal (i.p.) every week with 10 mg/kg of anti-EMP2 IgG1 antibody or a control IgG for 7 weeks. In a second experiment, 3 mice per group were treated with sequentially increasing concentrations of antibody beginning at 10 mg/kg, then 20 mg/kg, and finally 40 mg/kg twice a week. Weight was measured every week. At the end of the time course, mice were euthanized by cervical dislocation. Tissues (kidney, liver, spleen, lung, uterus, heart, ovary, and skin) were collected fixed in formalin, processed, embedded in paraffin, sectioned, stained with hematoxylin and eosin, and analyzed for pathologic changes by a pathologist (J. Braun). Complete blood counts and liver enzyme analysis (serum alanine aminotransferase, direct, and total bilirubin) were quantified by the UCLA Medical Center Clinical Laboratories.

Mouse xenograft model

To create tumor xenograft models, 4-to 6-week-old female BALB/c nude mice (Charles River Laboratories) were used for each condition. Briefly, 5×10^6 MDA-MB-468, 2×10^6 MDA-MD-231, or 2×10^7 Ramos cells were suspended in 5% Matrigel (BD Biosciences) and injected subcutaneously (s.c.) into the shoulder of female athymic mice. Tumor volume was calculated with the formula: length $\times$ width^2/2. When tumors reached 4 mm^3, they were injected intratumor (i.t.) with 1 mg/kg dose of anti-EMP2 diabody KS83 or control diabody twice a week as described previously (20). Alternatively, tumors were injected with 3 mg/kg i.t. or between 1 to 10 mg/kg systemically with anti-EMP2 IgG1 or control IgG (Sigma) every week as indicated in the figure legends. At the end of each experiment, tumors were isolated, fixed, and processed for hematoxylin and eosin staining as previously described (9).

Mouse metastatic model

To create a metastatic model for breast cancer, the spontaneous murine mammary tumor line 4T1 was used. A total of 1×10^4 4T1-FLUC cells were injected into the tail vein of BALB/c mice (Charles River Laboratories), using 9 mice per group. Before treatment, the presence of tumors was validated using bioluminescence. Mice were then

Published OnlineFirst January 21, 2014; DOI: 10.1158/1535-7163.MCT-13-0199

treated systemically twice, beginning at day 5, with 10 mg/kg anti-EMP2 IgG1 or control IgG. For bioluminescence imaging, mice received an intraperitoneal injection of 150 μL D-luciferin (30 mg/mL). Fifteen minutes after the injection of D-luciferin, the mice were anesthetized with isoflurane/oxygen and placed on the imaging stage. The bioluminescence signals were monitored using an IVIS-200 (Xenogen Corporation). The data were analyzed using the maximum photon flux emission (photons/second) in the regions of interest. After the final point, mice were euthanized and lungs isolated as above.

Statistical analysis

TMA analyses were performed as previously described (21, 30–33) using the Mann–Whitney test for two-group comparisons. A P value < 0.05 was considered significant. Differences in *in vitro* phenotypic changes or *in vivo* tumor growth were evaluated using a two-tailed Student unpaired t test at a 95% confidence level (GraphPad Prism version 3.0; GraphPad Software). P values < 0.05 were considered significant.

Results

EMP2 is upregulated in breast cancers

Numerous microarray studies have identified EMP2 mRNA as upregulated in breast cancer (18, 34, 35), and several studies have correlated its expression with advanced disease and metastasis (17, 19). Supplementary Table S1 provides a summary of these studies. However, to date, its protein expression has not been determined in breast cancer. Initially, the protein expression of EMP2 was quantitated by Western blot analysis and IHC in a small set of five flash-frozen human invasive ductal carcinoma samples and three samples of normal glandular breast epithelium. As shown in Fig. 1A, expression of EMP2 (18 kD) was elevated in breast cancer samples compared with normal tissue. To extend and validate these findings, the protein localization of EMP2 was assessed using IHC. Within malignant epithelium, EMP2 was predominantly present at the membrane and/or cytoplasm, whereas minimal/undetectable levels were observed in normal epithelium (Fig. 1B).

We further examined the expression profile of EMP2 in human breast cancer on a population basis using TMA technology. The demographic, clinical, and pathology characteristics are shown in Supplementary Table S2 and have been described previously (30–32). Compared with nonmalignant glandular and ductal mammary epithelium, there was a significant increase in EMP2 expression through disease progression. A significant increase in EMP2 expression was observed during stepwise progression of disease from normal to DCIS ($P < 0.0001$) as well as between invasive carcinoma and lymph node metastasis ($P = 0.012$; Fig. 1C). Within these groups, EMP2 expression was detectable in 63% of samples with invasive carcinoma ($n = 74$) with no correlation observed between EMP2 and hormone status or HER2/*neu* expression. EMP2 seemingly correlated with tumor progression as EMP2 was expressed in 67% of lymph node metastatic lesions ($n = 30$) with its expression correlating with lymphovascular invasion ($n = 13$; $P = 0.021$).

To further confirm EMP2 protein expression within breast tumors, its expression was determined in a panel of breast cancer cell lines (Fig. 1D). EMP2 was expressed in eight out of nine human cell lines tested by Western blot analysis with levels below detection in one cell line (HS578t). Within this panel of cell lines, EMP2 expression did not correlate with hormone and/or HER2/*neu* status as EMP2 expression was present in both triple-negative (MDA-MB-231, MDA-MB-468, and BT-20) and triple-positive (ZR-75-1) cells. EMP2 also exhibited high expression in all HER2/*neu*–positive cells tested (UACC812, SK-BR-3, BT-474).

As EMP2 was readily detectable within TNBC cell lines, its expression in TNBC tumors from the array was further considered. This group was of particular interest as TNBC is characterized by high recurrence, metastasis, and mortality rates (3, 36). Of the 11 patients with TNBC, 8 (73%) had relatively high expression levels of EMP2 while 3 cases had low or nondetectable levels (not shown). To independently validate the expression of EMP2 in TNBC, we further examined its expression in an additional independent set of 23 cases. Concordant with the TMA, 17 of 23 cases (74%) were positive for EMP2 (H score ≥ 1; see Supplementary Table S3).

Construction of the anti-EMP2 IgG1

In prior studies, we demonstrated the efficacy of recombinant anti-EMP2 diabody-mediated therapy in ovarian and endometrial cancers (7, 20). As EMP2 is widely expressed in breast cancer, we were prompted to assess the utility of targeting EMP2 in this malignancy as well. As diabodies tend to have a short half-life *in vivo* ($T_{1/2} = 6$ hours; ref. 37), we constructed a fully human anti-EMP2 IgG1 antibody to determine whether we could improve the therapeutic potential of targeting EMP2 using the variable heavy and variable light genes from the anti-EMP2 diabody clone KS49 (20). Anti-EMP2 IgG1 antibody was validated through sequencing (data not shown) and analyzed by SDS-PAGE under nonreducing and reducing conditions (Fig. 2A).

To characterize the specificity of the anti-EMP2 IgG1, its binding to an EMP2 peptide as well as to native protein was measured. Using a human EMP2 peptide, serial dilutions of the native antibody revealed an EC_{50} of 10.8 ng/mL (Fig. 2B). To further determine the binding characteristics of the anti-EMP2 IgG1, its binding to native EMP2 was assessed using flow cytometry. The anti-EMP2 IgG1 recognized both murine EMP2 present on 4T1 cells (Fig. 2C, top) and human EMP2 on the TNBC cell line MDA-MB-231 (Fig. 2C, bottom). Finally, the sensitivity and specificity of the antibody were confirmed. Anti-EMP2 IgG1 detected a difference in surface expression between HEC-1A wild-type and HEC-1A/EMP2 cells (Fig. 2D, top), which express a 2- to 4-fold increase in total EMP2 levels (15). Moreover, the binding of the

Published OnlineFirst January 21, 2014; DOI: 10.1158/1535-7163.MCT-13-0199

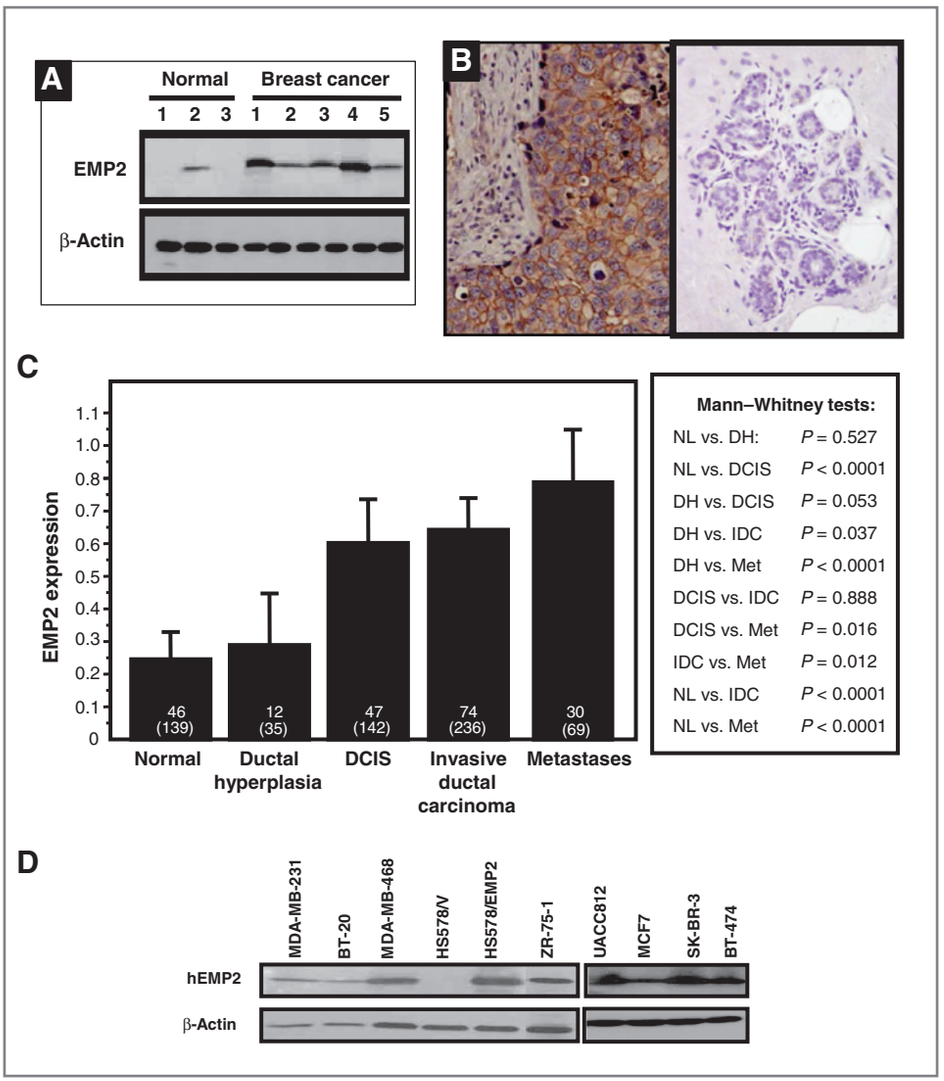

Figure 1. EMP2 expression is stratified by histologic type and stage. A, Western blot analysis was performed on whole tissue homogenates from normal and tumor regions of the breast. B, normal and breast cancer tissue were stained for EMP2 expression. Left, a representative patient with high EMP2 staining within a tumor is shown; Right, representative staining in normal breast. C, the mean integrated intensity of EMP2 protein expression for each category is shown using bar plots. Error bars, SEM. Top number, number of patients; bottom number in parenthesis, total number of spots tested. D, expression of EMP2 in a panel of breast cancer cell lines was evaluated by Western blot analysis. HS578/EMP2 cells were generated to stably overexpress EMP2. NL, normal; DH, ductal hyperplasia; IDC, invasive ductal carcinoma.

antibody was specific as it did not bind the EMP2-negative cell line Ramos (Fig. 2D, bottom).

To further confirm the binding specificity of the anti-EMP2 IgG1, the antibody was biotinylated and tested by IHC on tissue with known EMP2 expression (38). The anti-EMP2 IgG1 antibody recognized EMP2 on normal lung alveolar cells as well as on breast tumors. This binding was specific as peptide from the second extracellular loop of EMP2 blocked antigen recognition (Supplementary Fig. S1).

Anti-EMP2 treatment induces cell death *in vitro*

The therapeutic potential of the anti-EMP2 IgG1 was initially compared with the anti-EMP2 diabody. ZR-75-1, MDA-MB-468, HS578/V (the HS578t EMP2-negative TNBC cell line bearing an empty expression vector), and HS578t/EMP2 (bearing an EMP2 expression vector; ref. 15) were incubated *in vitro* with molar equivalent amounts of anti-EMP2 diabody, nonimmune Ctrl diabody, anti-EMP2 IgG1, or a saline control for 72 hours as described previously and monitored for viability (7, 20). Treatment of ZR-75-1, MDA-MB-468, and HS578/EMP2 cells with either anti-EMP2 diabody or anti-EMP2 IgG1 resulted in approximately 35% to 50% loss of viability compared with the control diabody or saline control (Fig. 3A). Treatment of HS578/V (EMP2-negative) cells with the anti-EMP2 diabody or anti-EMP2 IgG1 caused no loss in viability, indicating

Published OnlineFirst January 21, 2014; DOI: 10.1158/1535-7163.MCT-13-0199

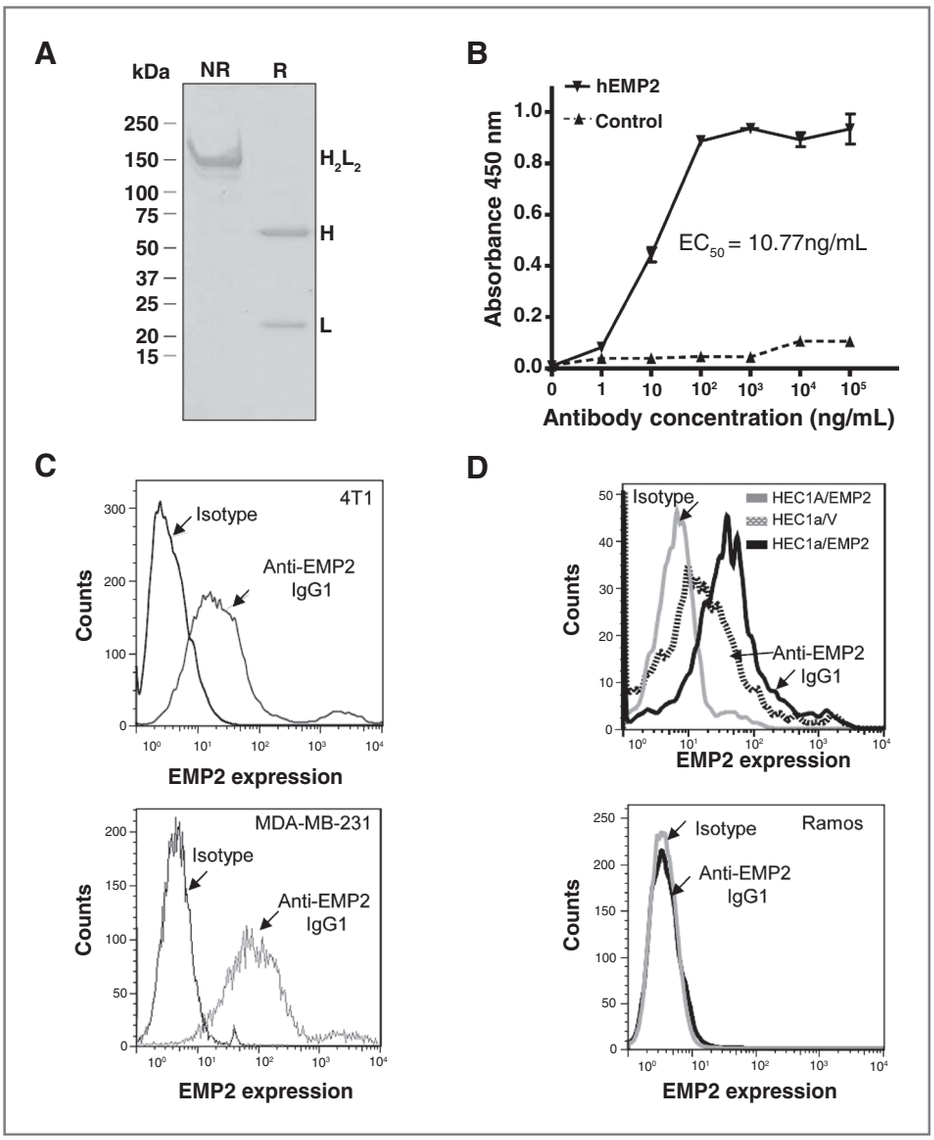

Figure 2. Characterization of recombinant anti-EMP2 IgG1. A, the anti-EMP2 IgG1 antibody was analyzed by SDS-PAGE under nonreducing (NR) and reducing (R) conditions. The full antibody structure is visualized under nonreducing conditions through a band around 150 kDa. This corresponds to the expected molecular weight for the anti-EMP2 IgG1. Under reducing conditions both the heavy chain (~60 kDa) and light chain (~20 kDa) are visualized. B, binding of the anti-EMP2 IgG1 to a human EMP2 peptide by ELISA. C, binding of anti-EMP2 IgG1 to both murine and human EMP2 by flow cytometry. Murine EMP2 was detected on the surface of murine mammary tumors (4T1 cells; top) or on MDA-MB-231 TNBC cells (bottom). D, the sensitivity and specificity of the anti-EMP2 IgG1 was determined by flow cytometry. Top, the sensitivity of the anti-EMP2 IgG1 to alternations in EMP2 expression was confirmed using HEC1a/EMP2 to endogenous levels of EMP2 (HEC1a/V). Bottom, the specificity was confirmed using an EMP2-negative cell line, human Ramos lymphoma cells.

that the effect was dependent on EMP2 expression (Fig. 3A).

To determine the sensitivity of a panel of breast cancer cells to EMP2 treatment, cells were treated with varying concentrations of anti-EMP2 IgG1 or control IgG (Fig. 3B). A dose-dependent reduction in cell viability was observed after 4 days in SK-BR-3, MDA-MB-231, and MDA-MB-468 cells. The respective sensitivity (IC_{50}) of the cell lines to anti-EMP2 IgG1 ranged from 2 μg/mL to 140 μg/mL for SK-BR-3 and MDA-MB-468, respectively. Importantly, no change in cellular viability was measured in EMP2-negative HS578t cells even at high concentrations of the antibody. As anti-EMP2 IgG1 recognized murine EMP2, we determined if the antibody could elicit a similar response in the 4T1 mouse mammary tumor line. 4T1 cells were susceptible to anti-EMP2 IgG1 with an IC_{50} of 108 μg/mL.

To determine if cell death occurred via apoptosis, cells were incubated with anti-EMP2 diabody or IgG1 (or appropriate controls) and then stained for Annexin V and

Published OnlineFirst January 21, 2014; DOI: 10.1158/1535-7163.MCT-13-0199

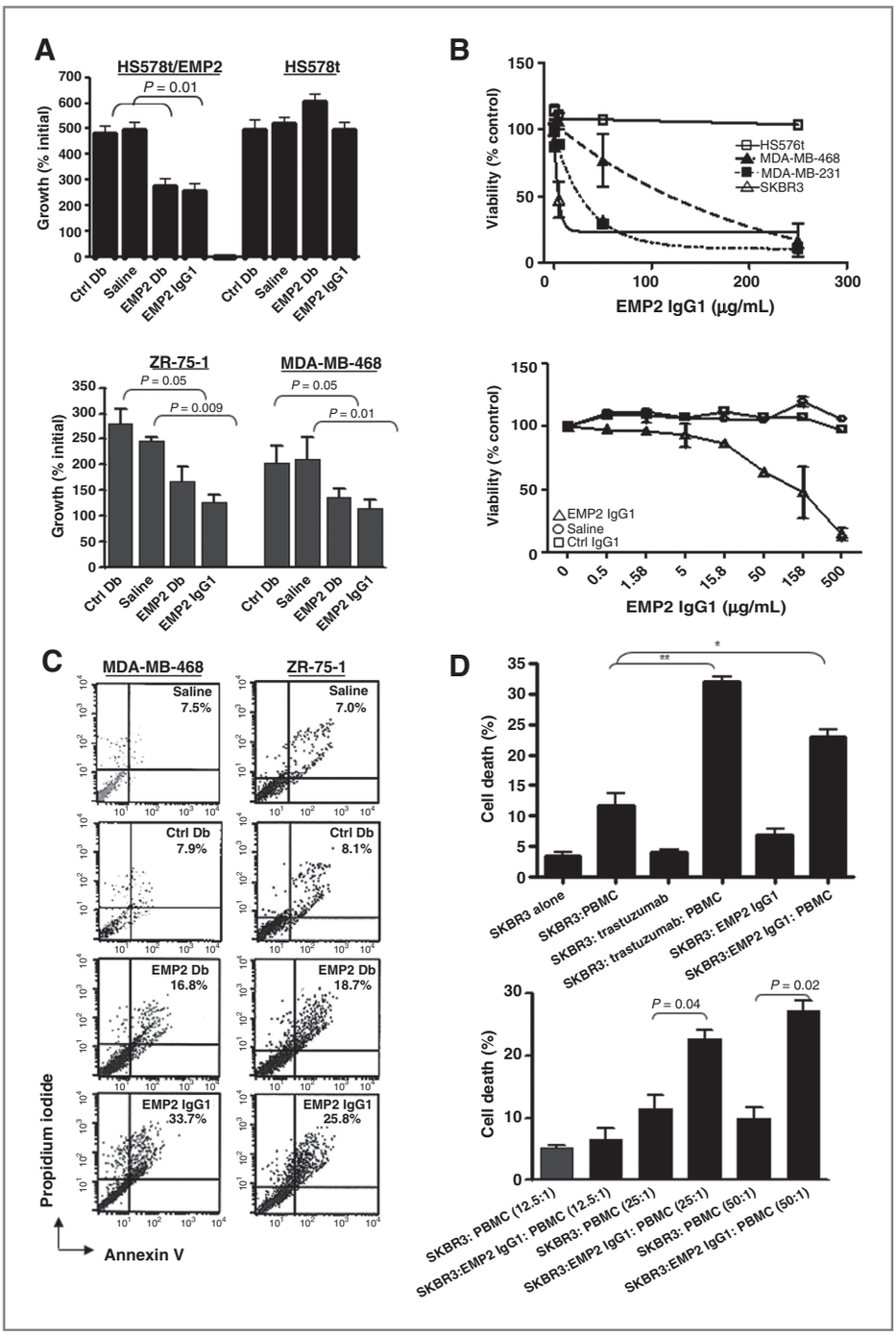

Figure 3. Anti-EMP2 IgG1 antibodies and diabodies (Db) induce cell death. A, top, HS578 cells do not express any endogenous EMP2 expression, and HS578/EMP2 cells were engineered to overexpress EMP2. Of note, 60 μg/mL anti-EMP2 IgG1, 20 μg/mL anti-EMP2Db, control diabody, or a vehicle control were added to the above cells for 72 hours. Cell growth, calculated as a percentage of the initial cells plated, was determined using trypan blue exclusion, and values represent results from three independent experiments (±SEM). Bottom, ZR-75-1 and MBA-MD-468 cells were treated for 72 hours as above to determine cell growth. Values are averages (±SEM; $n = 3$). B, SK-BR-3, MDA-MB-468, MDA-MB-231, and HS578t cells (top) or 4T1 cells (bottom) were incubated with increasing concentrations of anti-EMP2 IgG1 or control antibodies for up to 5 days. Cellular viability was assessed by the CellTiter-Glo Luminescent Cell Viability Assay. C, EMP2 diabodies and IgG1 promote apoptosis. ZR-75-1 (top) and MBA-MD-468 (bottom) cells were incubated with 20 μg/mL anti-EMP2 diabody, 20 μg/mL control diabody, 60 μg/mL anti-EMP2 IgG1, or 60 μg/mL control IgG. Cells were washed and stained with Annexin V and propidium iodide. Staining is expressed as the % Annexin V, propidium iodide–positive cells above the isotype control. The experiment was repeated three times with similar results. A representative graph is shown. D, *in vitro* anti-EMP2 IgG1-mediated ADCC against SK-BR-3 tumor cells. Top, SK-BR-3 cells were labeled with PKH67. Cells were mixed with freshly isolated PBMCs and/or 100 μg/mL trastuzumab or anti-EMP2 IgG1 (EMP2) at an effector/target ratio of 25:1. *, $P < 0.05$; **, $P < 0.01$. Bottom, SK-BR-3 cells were labeled with PKH67 and mixed at effector/target ratios of 12.5:1, 25:1, and 50:1 and/or 100 μg/mL anti-EMP2 IgG1. The percentage of killed cells was calculated as described in Materials and Methods.

Published OnlineFirst January 21, 2014; DOI: 10.1158/1535-7163.MCT-13-0199

by propidium iodide. As shown in Fig. 2C, incubation of ZR-75-1 or MDA-MB-468 cells with anti-EMP2 diabody or anti-EMP2 IgG1 induced apoptosis within 48 hours (Fig. 3C). Such an effect was not seen with the corresponding negative controls.

Anti-EMP2 IgG1 mediates ADCC against breast cancer cells

Although antibody treatment was able to directly induce apoptosis in EMP2-expressing breast cancer cells, we were curious as to whether such treatment might also elicit ADCC. We tested this effect *in vitro* using freshly isolated PBMCs and incubated them with the HER2-positive SK-BR-3 cell line. As shown in Fig. 3D (top and bottom), anti-EMP2 IgG1 treatment elicited a significant increase in cell death compared with the PBMC treatment alone. This ADCC effect was similar to that produced with trastuzumab.

Anti-EMP2 antibodies reduce tumor growth *in vivo*

To translate our *in vitro* data, we initially performed pharmacokinetic and toxicity studies to estimate a dosing schedule. Using C57B/6 mice, serum concentrations of trastuzumab and anti-EMP2 IgG1 after a single dose of 10 mg/kg were similar when measured over 1 week. For both antibodies, <5% of the antibody remained in circulation after 7 days (Supplementary Fig. S2). We previously have shown that weekly injections of EMP2 diabody demonstrated no detectable systemic toxicity or adverse host effects (7, 20). Likewise, upon extensive testing with weekly injections of the full-length anti-EMP2 IgG1 in C57B/6 mice (10 mg/kg) for 7 weeks or injections with increasing concentrations of antibody ranging from 10 mg/kg to 40 mg/kg, no indication of systemic or tissue-specific damage or toxicity was observed (Supplementary Tables 4 and 5, respectively). Comparison of weight, tissue histology, and pharmacologic parameters revealed no significant differences compared with control antibody treatment.

To determine the effectiveness of anti-EMP2 IgG1 *in vivo*, two mouse systems, a xenograft model and an orthotopic model of breast cancer metastasis, were used.

Subcutaneous xenograft tumor model

Two triple-negative cell lines were tested for their susceptibility to anti-EMP2 treatment. Initially, we tested a xenograft model involving the triple-negative cell line MDA-MB-468. Cells (2×10^6) were injected subcutaneously into nude BALB/c mice, and when tumors reached 4 mm^2 in size, anti-EMP2 diabody (1 mg/kg, twice a week) or the anti-EMP2 IgG1 (3 mg/kg, once a week) was injected directly into xenografts. A negative control diabody or saline was used as control treatments at the same dose and timing of treatment. As shown in Fig. 4A, treatment of tumors with anti-EMP2 diabody or anti-EMP2 IgG1 resulted in significant reduction of tumor growth by day 15 compared with controls. Upon histologic examination, tumors treated with anti-EMP2 diabody or IgG1 had extensive areas of necrosis in contrast with tumors treated with nonimmune reagents (Fig. 4A, bottom). To confirm that the ability of anti-EMP2 IgG1 to limit tumor growth was not dependent on localized injection, tumors were created from the MDA-MB-468 cell line as above but treated systemically. Anti-EMP2 IgG1 reduced tumor size (Fig. 4B) with extensive necrosis visible throughout the tumor (Fig. 4B, bottom).

We also examined the efficacy of anti-EMP2 IgG1 treatment on larger tumors (~200 mm^3) derived from another TNBC cell line, MDA-MB-231. Treatment with anti-EMP2 IgG1 significantly reduced tumor load by 50% compared with control IgG treatment (Fig. 4C) with tumors exhibiting pronounced necrosis (Fig. 4C, bottom). To validate that the effects of the anti-EMP2 IgG1 treatment were dependent on EMP2 expression, xenografts were created from the EMP2-negative B lymphoma cell line Ramos. Injection of anti-EMP2 IgG1 or control IgG1 showed no difference in tumor load (Fig. 4D) or in tumor histology (Fig. 4D, bottom).

Metastastic tumor model

Ninety percent of cancer-related mortality is caused by metastases formed by disseminated primary tumor cells at distant anatomic sites (39). Previous studies have suggested that EMP2 expression promotes FAK and Src activation, resulting in an increase in cellular migration and invasion (11). To validate that a similar effect occurs in breast cancer, MDA-MB-231 breast cancer cells were engineered to overexpress EMP2 or express a shRNA vector to knockdown expression. Similar to that observed in other models, EMP2 expression augmented cell migration, whereas shRNA knockdown reduced this effect (Fig. 5A). To correlate this change in migration with FAK and Src activation, a panel of breast cancer cells was tested for FAK and Src activation 24 hours after plating. Consistent with effects seen in endometrial cancer, upregulation of EMP2 promoted a significant increase in the activation of FAK and Src while the reciprocal effects were observed when EMP2 expression was reduced (Fig. 5B).

To determine whether EMP2 antibodies inhibit migration *in vitro*, MDA-MB-231 cells were treated with nontoxic doses of anti-EMP2 diabody or IgG1 with their appropriate antibody controls. Two-hour treatment with either anti-EMP2 diabody or IgG1 inhibited Transwell migration compared with the controls (Fig. 5C). When the mechanism behind this action was investigated, we observed that anti-EMP2 diabody or IgG1 significantly reduced Src phosphorylation (Fig. 5D). A modest reduction in FAK phosphorylation was also observed, but this effect was not significant (data not shown).

To determine the putative efficacy of anti-EMP2 IgG1 on metastatic tumors *in vivo*, 4T1/Fluc cells were injected intravenously into immunocompetent, syngeneic BALB/c hosts. Consistent with previous reports, these cells rapidly seed within the lungs, creating a model of late-stage metastatic disease (39, 40). Starting at day 5 post cell injection, mice were treated systemically twice

Published OnlineFirst January 21, 2014; DOI: 10.1158/1535-7163.MCT-13-0199

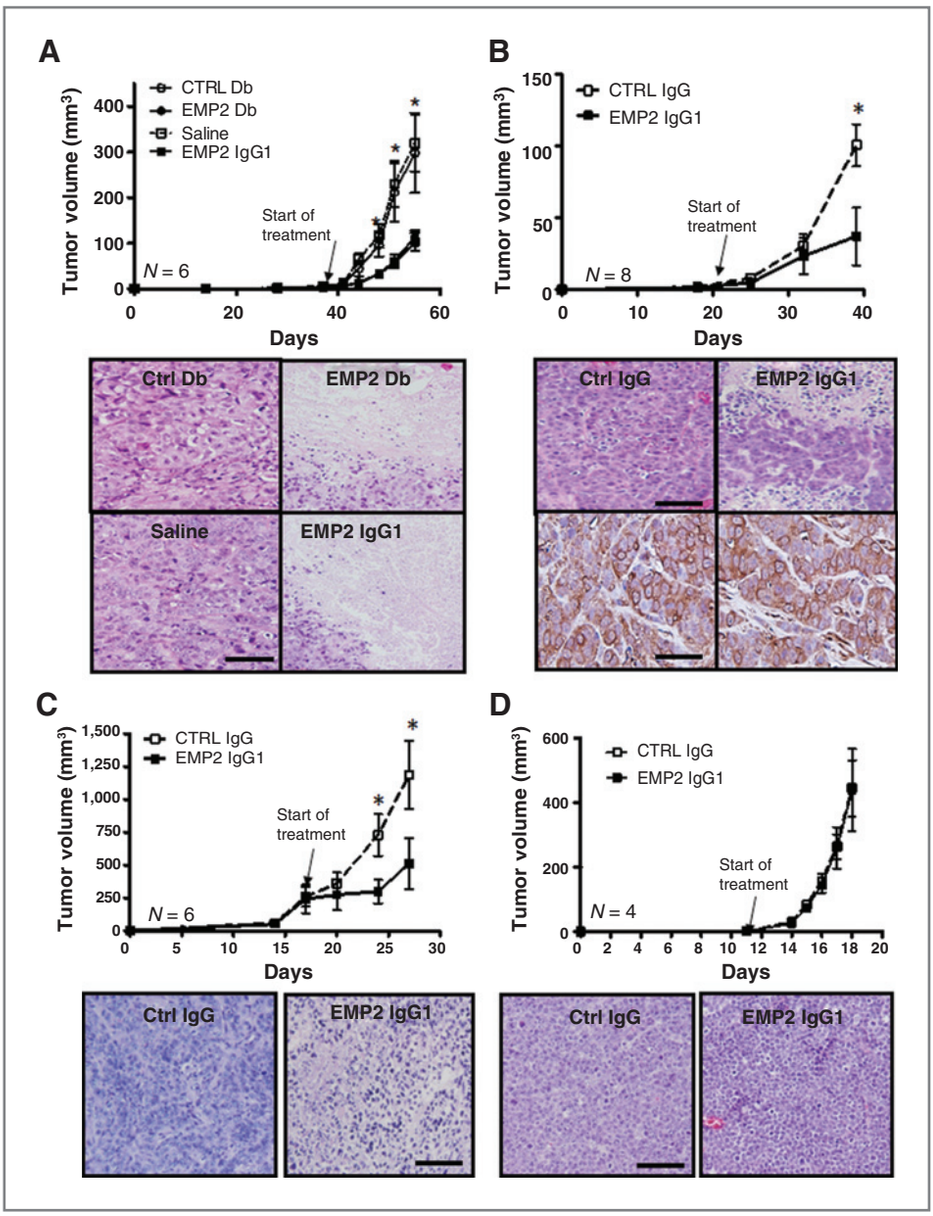

Figure 4. Targeting EMP2 reduces tumor load. A, MDA-MB-468 cells were injected subcutaneously into nude BALB/c female mice. Top, treatments were started when tumors reached 4 mm^3 (day 38). Tumors were injected intratumor with molar equivalent amounts of diabody (1 mg/kg), IgG1 antibody (3 mg/kg), or the indicated controls. Mice were injected twice a week, and tumor volume was monitored using calipers. Tumor volume values are averages (±SEM; $n = 6$ per group) with anti-EMP2 diabody and anti-EMP2 IgG1 treatment compared with control diabody and sterile saline, respectively. At day 56, tumors were excised, formalin fixed, and paraffin embedded. Bottom, tumor histology was assessed by hematoxylin and eosin staining. A representative image is shown on the right. B, MDA-MB-468 cells were injected into nude BALB/c mice as above. Top, tumors were treated when they reached 4 mm^3 (day 18), and mice were systemically treated with 10 mg/kg anti-EMP2 IgG1 or control IgG every week. Bottom, at day 38, tumor histology was assessed by hematoxylin and eosin staining as well as for residual EMP2 expression following treatment. $n = 6$ per group. C, MDA-MB-231 cells were injected into the mammary pad of BALB/c nude mice. When tumors reached approximately 250 mm^3 (day 16), mice were systemically injected with 10 mg/kg anti-EMP2 IgG1 or control IgG twice a week. Representative images of day 27 tumors stained with hematoxylin and eosin, right. $n = 6$ per group. D, Ramos cells were injected subcutaneously into nude BALB/c mice. As tumors grow rapidly, they were treated systemically twice in the week (day 0 and 3) with 10 mg/kg anti-EMP2 IgG1 or control IgG. Representative hematoxylin and eosin staining at day 28 is shown on the right. *, $P < 0.05$, comparison by the Student t test; image magnification, ×20; scale bar, 100 μm.

with 10 mg/kg, and at day 18, all mice were euthanized for further analyses. Biophotonic imaging of the animals before antibody treatment and after treatment reveal that anti-EMP2 IgG1 treatment slowed tumor growth with 6 of 8 (75%) mice following anti-EMP2 IgG1 treatment showing an exponential decrease in tumor load by imaging (Fig. 6A

Published OnlineFirst January 21, 2014; DOI: 10.1158/1535-7163.MCT-13-0199

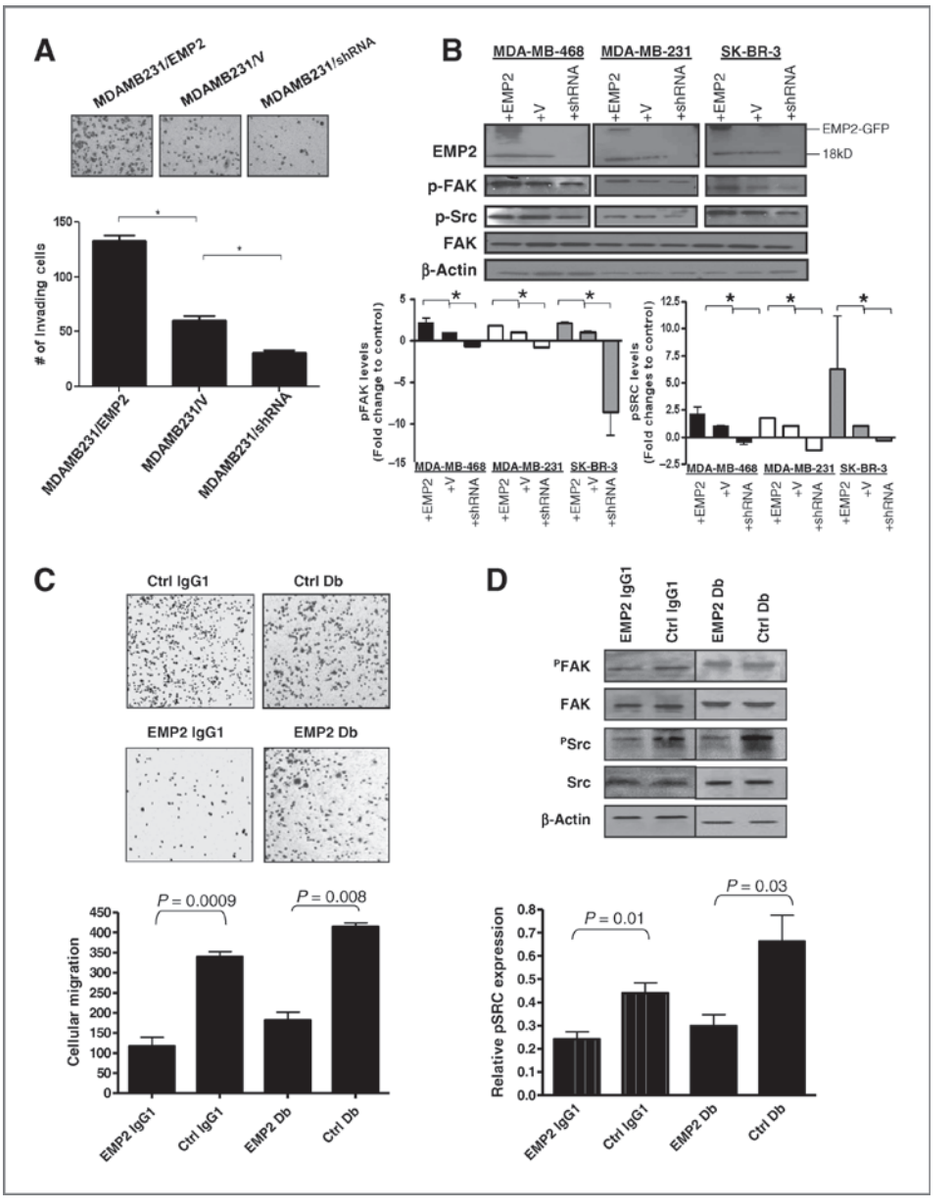

Figure 5. EMP2 promotes cellular migration and anti-EMP2 IgG1 antibodies and diabodies (Db) suppress this effect. A, MDA-MB-231 cells were engineered to overexpress EMP2 (MDAMB231/EMP2), express a vector control (MDAMB231/V) or reduce its expression via shRNA lentiviral vectors (MDAMB231/shRNA). Equivalent numbers of cells were plated into Transwells and enumerated after 6 hours. The experiment was repeated three times and the results were averaged. *, $P < 0.05$ as determined by the Student unpaired *t* test. B, MDA-MB-231, MDA-MB-468, and SK-BR-3 cells were engineered to overexpress or reduce EMP2 expression as above. Cells were plated for 12 hours and FAK and Src activation were assessed by Western blot analysis. $n = 3$; *, $P < 0.05$, Student unpaired *t* test. C, 60 μg/mL anti-EMP2 IgG1 or control IgG or 20 μg/mL anti-EMP2 or control diabody were added to MDA-MB-468 cells for 1 hour. The number of cells that migrated through the Transwell was measured. Top, cells were visualized using crystal violet. Bottom, averaged number of migrated cells from three experiments. D, 60 μg/mL anti-EMP2 IgG1 or control IgG was added to MDA-MB-468 cells for 1 hour. Alternatively, 20 μg/mL anti-EMP2 or control diabody were added. Cells were then plated for 12 hours and lysed. Proteins were separated by SDS-PAGE and probed using the indicated antibodies. The experiment was repeated three times, and representative image is shown. Bottom, activated pSRC expression from three experiments was quantified using ImageJ, and the data were normalized relative to total Src levels. Treatment with anti-EMP2 IgG1 or anti-EMP2 diabody significantly reduced pSRC expression. Values are averages (±SEM).

and B). When tumors were removed and evaluated by IHC, all mice treated with anti-EMP2 IgG1 showed an increase in necrosis throughout the tumor (Fig. 6C). Importantly, the normal mouse lung parenchyma and stroma showed no pathology due to anti-EMP2 IgG1 therapy.

Discussion

In this study, we examined the expression levels of EMP2 in breast cancer and found that it was expressed in 63% of invasive ductal carcinomas tested with low to minimal expression in normal mammary glandular and

Published OnlineFirst January 21, 2014; DOI: 10.1158/1535-7163.MCT-13-0199

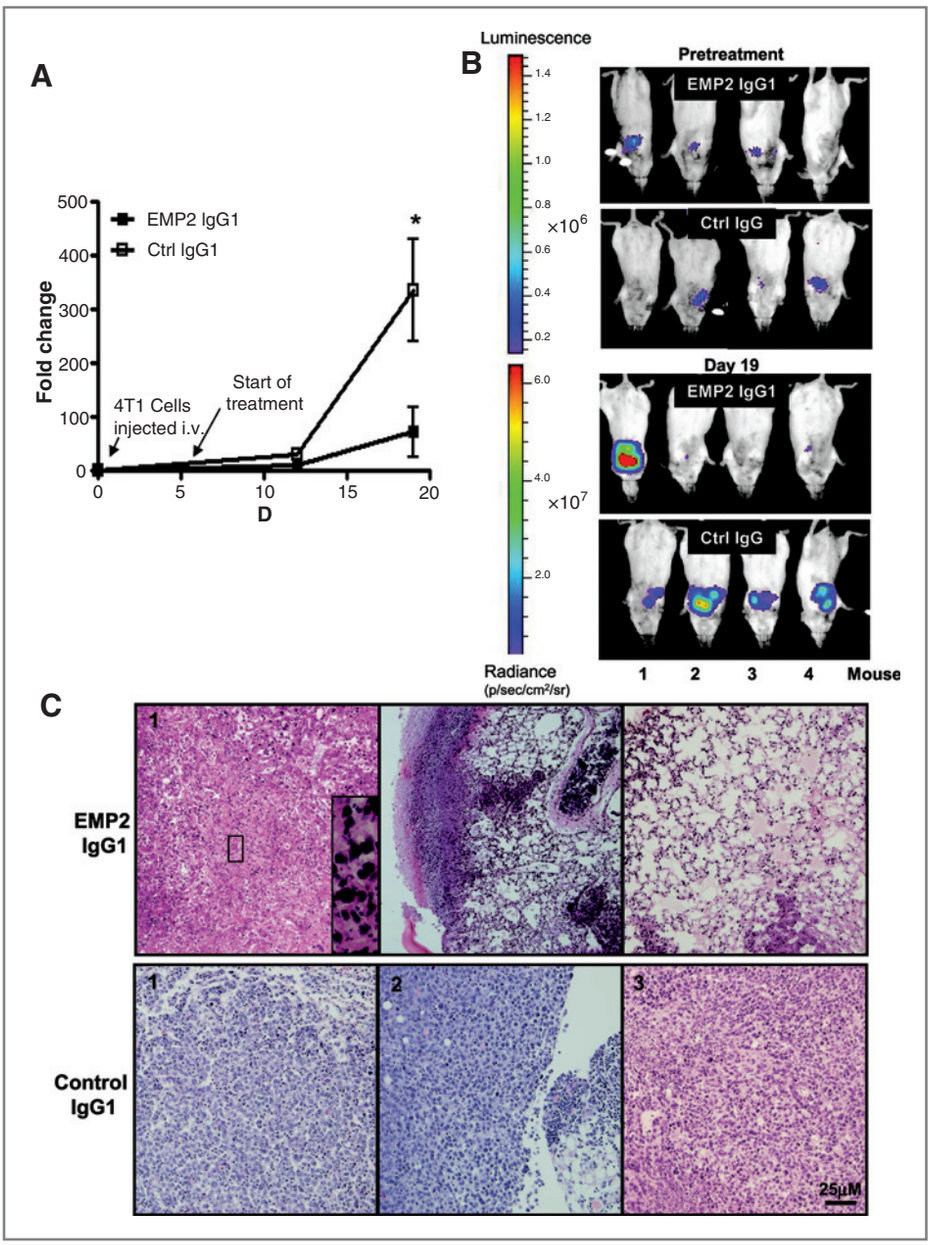

Figure 6. Anti-EMP2 IgG1 antibodies reduce tumor load in a 4T1 lung metastatic model. A, 4T1-FLUC cells were injected into the tail vein of nude BALB/c mice. Mice were treated systemically with 10 mg/kg EMP2 IgG1 or Ctrl IgG twice a week, and tumor load was monitored. $n = 9$ per group; *, $P = 0.02$, comparison by the Student t test. B, 5 days after cell injection but before treatment, luciferase activity was monitored, showing localization of cells into the lungs of all mice. Following three treatments with anti-EMP2 IgG1 or Ctrl IgG (day 18), tumor load was measured by bioluminescence. C, at day 18, all mice were euthanized, and lungs were examined by hematoxylin and eosin staining. Representative images from 4 mice are shown. Image magnification, ×20; insets, ×140 magnification; scale bar, 25 μm.

ductal cells. Of significance, greater than 70% of TNBC cases from two independent cohorts of patients expressed EMP2. This is of particular interest, given that TNBC, although accounting for 20% to 30% of all breast cancer cases, is associated with high mortality rates as these patients show a high recurrence of residual disease within 3 years (41). Moreover, high EMP2 expression was observed in lymph node metastatic lesions. Given that an estimated 90% of deaths due to breast cancer are a consequence of metastatic disease, the identification of a new molecular target to specifically target these types of tumors is of high importance. Importantly, our results are concordant with several studies showing that EMP2 mRNA is upregulated in breast cancer and that its expression correlates with advanced and metastatic disease. Thus, its expression profile and localization on the plasma membrane make EMP2 an attractive target for passive immunotherapy with recombinant monoclonal antibodies.

Of note, treatment of proliferating EMP2-expressing malignant cells with anti-EMP2 IgG1 promoted cell death with resultant reductions in tumor load in both human xenograft and murine metastatic models. Our results suggest that anti-EMP2 IgG1 elicits cell death both directly as well as through an ADCC response. Although the exact mechanism for direct cytotoxicity is still being elucidated, the known cell biology of EMP2 may provide insight. Previous studies have shown that

Published OnlineFirst January 21, 2014; DOI: 10.1158/1535-7163.MCT-13-0199

EMP2 associates with and regulates the localization and activity of select integrin pairs (15, 42), and it has been shown to promote the phosphorylation of both FAK and Src in a number of normal and malignant cells (11, 12). In this study, we show that in breast cancer, EMP2 levels correlate with FAK and Src activation and promote invasion *in vitro*, and treatment with anti-EMP2 diabody or IgG1 reduces phosphorylation of Src within 12 hours of administration. This may be important as groups have linked Src activation to breast cancer survival, metastasis, as well as trastuzumab resistance (43–45). Correspondingly, several groups have shown that a reduction in Src leads to programmed cell death in breast cancer (46). Hence, the reduction in Src activation by anti-EMP2 IgG1 may provide a plausible explanation for the cell death elicited by the antibody.

The anti-EMP2 IgG1 cross-reacts with human and murine EMP2, and we have previously shown using normal human tissue arrays and murine sections that both species have a similar tissue distribution (38). Although EMP2 is not ubiquitously expressed, it is present in a number of discrete locations in mice and humans such as normal lung type 1 pneumocytes (47), the retinal pigmented epithelium of the eye (28), and secretory epithelium of the endometrium (9). Nevertheless, in healthy mice injected with 10 mg/kg every week of anti-EMP2 IgG1 for up to 2 months showed no obvious adverse effects as gaged by animal weight and health, tissue histology, and the release of liver serum proteins. Moreover, treatment of up to 40 mg/kg also did not elicit any measurable toxicity. Indeed, to date, we have found no evidence of toxicity following chronic systemic treatment with anti-EMP2 IgG1 *in vivo*.

Over the last 2 decades, the use of monoclonal antibodies for cancer therapy has achieved considerable success. In breast cancer, trastuzumab has changed the standard-of-care for women with cancers overexpressing HER2/*neu*, and remains one of the few U.S. Food and Drug Administration (FDA)–approved options for women with metastatic breast cancer (48, 49). Our findings offer proof-of-concept for the use of anti-EMP2 IgG1 as an effective therapy for breast cancer. Although anti-EMP2 IgG1 reduced tumor load between 50% and 80% in all three breast cancer models tested *in vivo*, we recognize that like all targeted therapies, anti-EMP2 IgG1 may need to be used in combination with other drugs. Although we are currently investigating the best combinations of drugs to pair with anti-EMP2 IgG1, studies suggest that its mRNA expression in breast cancer is retained following standard chemotherapy (19). Thus, the biologic properties and expression profile of EMP2, elucidated by the preclinical studies presented previously and here, suggest that this fully human, full-length antibody has the potential to be a first-in-class, effective therapeutic for the treatment of EMP2-dependent cancers.

Conclusions

These results present compelling evidence that EMP2 is highly expressed in TNBC as well as in other breast cancer variants. Antibodies and antibody fragments to EMP2 reduce tumor load in animal models, suggesting that EMP2 is a novel therapeutic target in TNBC and other forms of breast cancer.

Disclosure of Potential Conflicts of Interest

L.K. Gordon and M. Wadehra have ownership interest (including patents) in Paganini Biopharma. J. Braun has ownership interest (including patents) in and is a member of the board of directors of Paganini Biopharma. No potential conflicts of interest were disclosed by the other authors.

Authors' Contributions

Conception and design: L.K. Gordon, J. Braun, M.L. Penichet, L. Goodglick, M. Wadehra
Development of methodology: M. Fu, G.F. Helguera, Y. Qin, T.R. Daniels-Wells, N. Aziz, R.A. Soslow, M.L. Penichet, M. Wadehra
Acquisition of data (provided animals, acquired and managed patients, provided facilities, etc.): M. Fu, G.F. Helguera, M. Kiyohara, Y. Qin, N. Ashki, L.K. Gordon, Y. Elshimali, M.L. Penichet, L. Goodglick, M. Wadehra
Analysis and interpretation of data (e.g., statistical analysis, biostatistics, computational analysis): M. Fu, E.L. Maresh, M. Kiyohara, Y. Qin, N. Ashki, T.R. Daniels-Wells, L.K. Gordon, J. Braun, Y. Elshimali, R.A. Soslow, M.L. Penichet, L. Goodglick, M. Wadehra
Writing, review, and/or revision of the manuscript: Y. Qin, T.R. Daniels-Wells, L.K. Gordon, J. Braun, Y. Elshimali, M.L. Penichet, L. Goodglick, M. Wadehra
Administrative, technical, or material support (i.e., reporting or organizing data, constructing databases): M. Kiyohara, Y. Qin, N. Aziz, M.L. Penichet, M. Wadehra
Study supervision: M.L. Penichet, L. Goodglick, M. Wadehra

Acknowledgments

The authors thank Lin Lin for helpful discussions on the ADCC experiments and Dr. Sheri Morrison (University of California, Los Angeles) for providing the antibody expression vectors.

Grant Support

This work is supported by the Early Detection Research Network NCI CA-86366 (to L. Goodglick), a Charles Drew University/UCLA NIH grant (U54-CA-143931; to M. Wadehra), R01 CA163971 (to M. Wadehra), K01-CA138559 (to T.R. Daniels-Wells), P30 CA016042 (to the UCLA Jonsson Comprehensive Cancer Center Flow Cytometry Core), NCRR and NCATS UL1TR000124 (to UCLA Clinical Translational Science Institute), the Stein Oppenheimer Seed Grant (to M. Wadehra), ANPCyT-FONARSEC PICT-PRH 2008-00315 (to G.F. Helguera), CONICET PIP Nº 114-2011-01-00139 (to G.F. Helguera), and UBACYT Nº 200-2011-02-00027 (to G.F. Helguera).

The costs of publication of this article were defrayed in part by the payment of page charges. This article must therefore be hereby marked *advertisement* in accordance with 18 U.S.C. Section 1734 solely to indicate this fact.

Received March 20, 2013; revised October 1, 2013; accepted January 15, 2014; published OnlineFirst January 21, 2014.

References

1. Higgins MJ, Baselga J. Targeted therapies for breast cancer. J Clin Invest 2011;121:3797–803.
2. Elias AD. Triple-negative breast cancer: a short review. Am J Clin Oncol 2010;33:637–45.
3. Foulkes WD, Smith IE, Reis-Filho JS. Triple-negative breast cancer. N Engl J Med 2010;363:1938–48.
4. Weigelt B, Peterse JL, van 't Veer LJ. Breast cancer metastasis: markers and models. Nat Rev Cancer 2005;5:591–602.

Published OnlineFirst January 21, 2014; DOI: 10.1158/1535-7163.MCT-13-0199

5. Siegel R, Naishadham D, Jemal A. Cancer statistics, 2012. CA Cancer J Clin 2012;62:10–29.
6. Ferlay J, Shin H-R, Bray F, Forman D, Mathers C, Parkin DM. Estimates of worldwide burden of cancer in 2008: GLOBOCAN 2008. Int J Cancer 2010;127:2893–917.
7. Fu M, Maresh EL, Soslow RA, Alavi M, Mah V, Zhou Q, et al. Epithelial membrane protein-2 is a novel therapeutic target in ovarian cancer. Clin Cancer Res 2010;16:3954–63.
8. Habeeb O, Goodglick L, Soslow RA, Rao RG, Gordon LK, Schirripa O, et al. Epithelial membrane protein-2 expression is an early predictor of endometrial cancer development. Cancer 2010;116:4718–26.
9. Wadehra M, Natarajan S, Seligson DB, Williams CJ, Hummer AJ, Hedvat C, et al. Expression of epithelial membrane protein-2 is associated with endometrial adenocarcinoma of unfavorable outcome. Cancer 2006;107:90–8.
10. Gordon LK, Kiyohara M, Fu M, Braun J, Chan AM, Goodglick L, et al. EMP2 regulates angiogenesis in endometrial cancer cells through induction of VEGF. Oncogene 2013;32:5369–76.
11. Fu M, Rao R, Sudhakar D, Hogue CP, Rutta Z, Morales S, et al. Epithelial membrane protein-2 promotes endometrial tumor formation through activation of FAK and Src. PLoS ONE 2011;6:e19945.
12. Morales SA, Mareninov S, Coulam P, Wadehra M, Goodglick L, Braun J, et al. Functional consequences of interactions between FAK and epithelial membrane protein 2 (EMP2). Invest Ophthalmol Vis Sci 2009;50:4949–56.
13. Morales SA, Mareninov S, Prasad P, Wadehra M, Braun J, Gordon LK. Collagen gel contraction by ARPE-19 cells is mediated by a FAK-Src dependent pathway. Exp Eye Res 2007;85:790–8.
14. Morales SA, Mareninov S, Wadehra M, Zhang L, Goodglick L, Braun J, et al. FAK activation and the role of epithelial membrane protein 2 (EMP2) in collagen gel contraction. Invest Ophthalmol Vis Sci 2009;50:462–9.
15. Wadehra M, Forbes A, Pushkarna N, Goodglick L, Gordon LK, Williams CJ, et al. Epithelial membrane protein-2 regulates surface expression of alphavbeta3 integrin in the endometrium. Dev Biol 2005;287:336–45.
16. van 't Veer LJ, Dai H, van de Vijver MJ, He YD, Hart AA, Mao M, et al. Gene expression profiling predicts clinical outcome of breast cancer. Nature 2002;415:530–6.
17. Obermayr E, Sanchez-Cabo F, Tea MK, Singer CF, Krainer M, Fischer MB, et al. Assessment of a six gene panel for the molecular detection of circulating tumor cells in the blood of female cancer patients. BMC Cancer 2010;10:666.
18. Kao J, Salari K, Bocanegra M, Choi YL, Girard L, Gandhi J, et al. Molecular profiling of breast cancer cell lines defines relevant tumor models and provides a resource for cancer gene discovery. PLoS ONE 2009;4:e6146.
19. Watson MA, Ylagan LR, Trinkaus KM, Gillanders WE, Naughton MJ, Weilbaecher KN, et al. Isolation and molecular profiling of bone marrow micrometastases identifies TWIST1 as a marker of early tumor relapse in breast cancer patients. Clin Cancer Res 2007;13:5001–9.
20. Shimazaki K, Lepin EJ, Wei B, Nagy AK, Coulam CP, Mareninov S, et al. Diabodies targeting epithelial membrane protein 2 reduce tumorigenicity of human endometrial cancer cell lines. Clin Cancer Res 2008;14:7367–77.
21. Yoon NK, Seligson DB, Chia D, Elshimali Y, Sulur G, Li A, et al. Higher expression levels of 14-3-3sigma in ductal carcinoma in situ of the breast predict poorer outcome. Cancer Biomark 2009;5:215–24.
22. Presson AP, Yoon NK, Bagryanova L, Mah V, Alavi M, Maresh EL, et al. Protein expression based multimarker analysis of breast cancer samples. BMC Cancer 2011;11:230.
23. Xuan C, Steward KK, Timmerman JM, Morrison SL. Targeted delivery of interferon-alpha via fusion to anti-CD20 results in potent antitumor activity against B-cell lymphoma. Blood 2010;115:2864–71.
24. Helguera G, Penichet ML. Antibody-cytokine fusion proteins for the therapy of cancer. Methods Mol Med 2005;109:347–74.
25. Qu Z, Griffiths GL, Wegener WA, Chang C-H, Govindan SV, Horak ID, et al. Development of humanized antibodies as cancer therapeutics. Methods 2005;36:84–95.
26. Morrison SL, Wims L, Wallick S, Tan L, Oi VT. Genetically engineered antibody molecules and their application. Ann N Y Acad Sci 1987;507:187–98.
27. Wadehra M, Sulur GG, Braun J, Gordon LK, Goodglick L. Epithelial Membrane Protein-2 is expressed in discrete anatomical regions of the eye. Exp Mol Pathol 2003;74:106–12.
28. Colello D, Mathew S, Ward R, Pumiglia K, LaFlamme SE. Integrins regulate microtubule nucleating activity of centrosome through mitogen-activated protein kinase/extracellular signal-regulated kinase kinase/extracellular signal-regulated kinase (MEK/ERK) signaling. J Biol Chem 2012;287:2520–30.
29. Zhang SQ, Yang W, Kontaridis MI, Bivona TG, Wen G, Araki T, et al. Shp2 regulates SRC family kinase activity and Ras/Erk activation by controlling Csk recruitment. Mol Cell 2004;13:341–55.
30. Yoon NK, Maresh EL, Elshimali Y, Li A, Horvath S, Seligson DB, et al. Elevated MED28 expression predicts poor outcome in women with breast cancer. BMC Cancer 2010;10:335.
31. Yoon NK, Maresh EL, Shen D, Elshimali Y, Apple S, Horvath S, et al. Higher levels of GATA3 predict better survival in women with breast cancer. Hum Pathol 2010;41:1794–801.
32. Shen D, Nooraie F, Elshimali Y, Lonsberry V, He J, Bose S, et al. Decreased expression of annexin A1 is correlated with breast cancer development and progression as determined by a tissue microarray analysis. Hum Pathol 2006;37:1583–91.
33. Mah V, Seligson DB, Li A, Marquez DC, Wistuba II, Elshimali Y, et al. Aromatase expression predicts survival in women with early-stage non small cell lung cancer. Cancer Res 2007;67:10484–90.
34. Zhao H, Langerød A, Ji Y, Nowels KW, Nesland JM, Tibshirani R, et al. Different gene expression patterns in invasive lobular and ductal carcinomas of the breast. Mol Biol Cell 2004;15:2523–36.
35. Ma X-J, Dahiya S, Richardson E, Erlander M, Sgroi D. Gene expression profiling of the tumor microenvironment during breast cancer progression. Breast Cancer Res 2009;11:R7.
36. Pal SK, Childs BH, Pegram M. Triple negative breast cancer: unmet medical needs. Breast Cancer Res Treat 2011;125:627–36.
37. Holliger P, Prospero T, Winter G. "Diabodies": small bivalent and bispecific antibody fragments. Proc Natl Acad Sci U S A 1993;90:6444–8.
38. Fu M, Brewer S, Olafsen T, Wu A, Gordon L, Said J, et al. Positron emission tomography imaging of endometrial cancer using engineered anti-EMP2 antibody fragments. Mol Imaging Biol 2013;15:68–78.
39. Ma L, Reinhardt F, Pan E, Soutschek J, Bhat B, Marcusson EG, et al. Therapeutic silencing of miR-10b inhibits metastasis in a mouse mammary tumor model. Nat Biotech 2010;28:341–7.
40. Yang J, Mani SA, Donaher JL, Ramaswamy S, Itzykson RA, Come C, et al. Twist, a master regulator of morphogenesis, plays an essential role in tumor metastasis. Cell 2004;117:927–39.
41. Hortobagyi GN. Toward individualized breast cancer therapy: translating biological concepts to the bedside. Oncologist 2012;17:577–84.
42. Wadehra M, Iyer R, Goodglick L, Braun J. The tetraspan protein epithelial membrane protein-2 interacts with beta1 integrins and regulates adhesion. J Biol Chem 2002;277:41094–100.
43. Burgess DJ. Breast cancer: SRC hits the mark. Nat Rev Cancer 2011;11:314–5.
44. Zhang S, Huang W-C, Li P, Guo H, Poh S-B, Brady SW, et al. Combating trastuzumab resistance by targeting SRC, a common node downstream of multiple resistance pathways. Nat Med 2011;17:461–9.
45. Zhang XHF, Wang Q, Gerald W, Hudis CA, Norton L, Smid M, et al. Latent bone metastasis in breast cancer tied to Src-dependent survival signals. Cancer Cell 2009;16:67–78.
46. Rucci N, Recchia I, Angelucci A, Alamanou M, Del Fattore A, Fortunati D, et al. Inhibition of protein kinase c-Src reduces the incidence of breast cancer metastases and increases survival in mice: implications for therapy. J Pharmacol Exp Ther 2006;318:161–72.
47. Dahlin K, Mager EM, Allen L, Tigue Z, Goodglick L, Wadehra M, et al. Identification of genes differentially expressed in rat alveolar type I cells. Am J Respir Cell Mol Biol 2004;31:309–16.
48. Nahta R, Yu D, Hung M-C, Hortobagyi GN, Esteva FJ. Mechanisms of Disease: understanding resistance to HER2-targeted therapy in human breast cancer. Nat Clin Prac Oncol 2006;3:269–80.
49. Vanneman M, Dranoff G. Combining immunotherapy and targeted therapies in cancer treatment. Nat Rev Cancer 2012;12:237–51.